SACLANTCEN REPORT
serial no: SR- 348

SACLANT UNDERSEA RESEARCH CENTRE REPORT

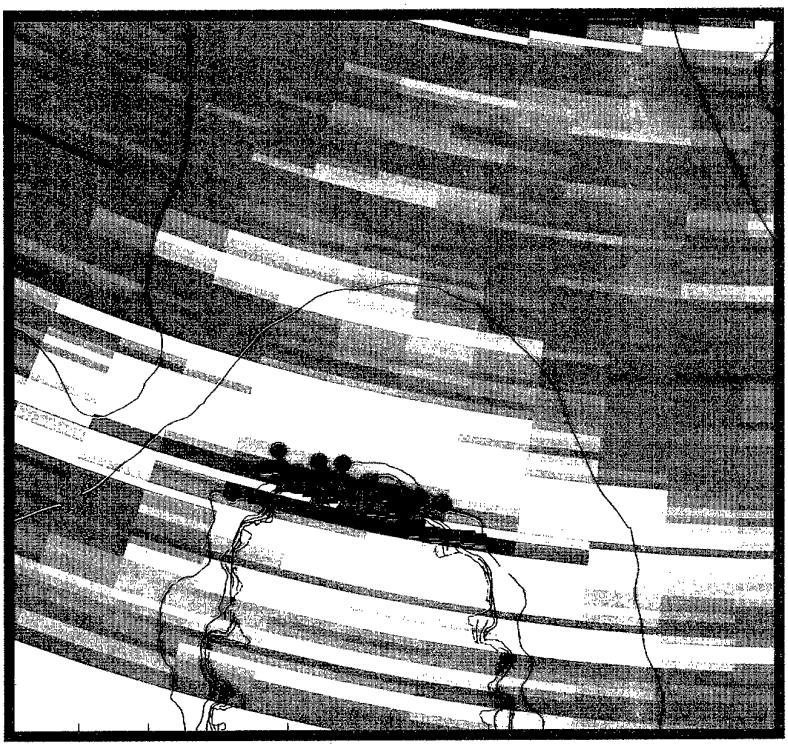

NORTH ATLANTIC TREATY ORGANIZATION ORGANISATION DU TRAITE DE L'ATLANTIQUE NORD

SACLANTCEN SR-348

Reverberation consistency: DUSS-97 data

R. Laterveer and S. Bongi

The content of this document pertains to work performed under Project 04-AB of the SACLANTCEN Programme of Work. The document has been approved for release by The Director, SACLANTCEN.

Jan L. Spoelstra
Director

intentionally blank page

Reverberation consistency: DUSS-97 data

R. Laterveer and S. Bongi

Executive Summary:

Low frequency active sonar has been highlighted by a number of NATO nations as an important component of the next generation of undersea defence systems. The use of low frequencies in a shallow water environment, however, is known to result in a high false alarm rate due to the large number of reverberation returns which can overload automatic tracking and classification algorithms.

The SACLANT Undersea Research Centre is currently investigating techniques to aid in the reduction of these false alarms without a reduction in detection probability.

To remove reverberation returns a single detection opportunity is usually not enough. Observations over time or from more than one receiving station must be combined to discriminate reverberation from true target returns.

We study the stability of reverberation features as a function of time, frequency and receiving station. We use data gathered during a multi-static experiment in a setup of a single source and three fixed receiving stations.

The main conclusion is that to associate detections over station and time accurate geographical mapping of the data is essential. Therefore fixed buoys should have accurate calibrated compasses.

Future work will concentrate on data from advanced towed array experiments.

intentionally blank page

Reverberation consistency: DUSS-97 data

R. Laterveer and S. Bongi

Abstract:

The use of low frequency active sonar in shallow water leads to large numbers of reverberation detections which can overload automatic tracking and classification algorithms.

We study the stability of reverberation returns from the DUSS97 multi-static experiment using fixed buoys.

The main conclusion is that to associate detections over station and time accurate geographical mapping of the data is essential. Therefore fixed buoys should have accurate calibrated compasses.

Keywords: Low Frequency Active Sonar ○ Multi Frequency Sonar ○ Multi-static Sonar ○ Reverberation ○ Compass

Contents

1
Introduction

The expected arena of use for active ASW has moved from large deep-water areas to smaller shallow and coastal waters. When used in these types of environment, deep-water oriented active sonars do not perform as well because of the predominance of harsh environmental conditions with which they are confronted. The main environmental challenge comes from reverberation.

Diffuse bottom reverberation can reduce the probability of detection by presenting acoustic background energy that obscures the target echo in the same observation cell. This type of reverberation is typically seen close-in, immediately after the reception of the direct blast, as well as from more distant seamounts, ridges, coastlines, or other high profile scattering areas.

Reverberation clutter increases the probability of false alarm. This occurs when confusing "target-like" reverberation echoes pass through the detector in neighboring observation cells. These false alarms can be attributed to smaller scale bottom and sub-bottom features, gas pockets and wrecks.

The use of broadband sonar is expected to be attractive for reverberation/clutter reduction and classification. It reduces reverberation, offers environmentally adaptable frequency selectivity, and increases classification potential. Also, broadband sources and receivers improve the interoperability needed for multi-platform and multi-static operations.

Another technique is multi-statics where data from multiple sensors are combined. These systems consist of one or more sources and multiple receivers. This allows multiple simultaneous views of a target and target-like features and shows potential to improve the performance of the sonar system.

In order to exploit these techniques we have to know how clutter behaves as a function of the parameters like frequency, aspect and muli-static station. This knowledge can then be used to determine contact features allowing to eliminate target-like clutter. The relevant parameters include:

- Frequency
  Scattering is frequency dependent so choosing an optimal frequency can reduce

target-like clutter while maintaining high target detection probability.

- Aspect
  The target scattering response is highly dependent on the aspect angle of the incoming sound while scattering from non man made objects usually vary only slowly on aspect angle.

- Multi-statics
  A target cannot reduce it's scattering response in multiple directions simultaneously so when using multi-statics will likely show a much larger response on one of the receivers. Geo-acoustical target-like objects on the other hand usually show roughly equal levels on all receivers.

- Ping to ping
  Ping to ping consistency of clutter will allow it to designated as fixed and consequently removed. This is called fixed-feature removal.

Not all aspects can be studied with the data set used for this report. Future work will study additional aspects of clutter consistency.

One can distinguish two different approaches towards studying clutter. There is the fundamental approach which studies the physical processes, like bottom and subbottom scattering, underlying clutter. From this understanding one tries to deduce clues to distinguish clutter from real target detections.

Our approach is more phenomenological in nature. We study clutter as it is produced and received by the sonar system. Therefore all effects, including scattering, propagation and equipment related are taken into account.

Section 2 describes the experiment whose data we analyze. In Sect. 3.1 the signal processing used is given while Sect. 4 shows the results and discusses some of the findings. We finish in Sect. 5 with some conclusions and recommendations.

2
Experiment

In this report we study data from the DUSS '97 experiment. The acronym DUSS stands for Deployable Underwater Surveillance Systems, a multi-static system of small buoys which can cover an area [1]. The experiment was executed in 1997 south of the Island of Elba (Italy). Figure 1 shows a geographical map of the area and the deployment geometry of the sonar elements.

The data contains measurements from three receiving stations positioned on a straight line at 2 nm spacing. The first station, a (quasi-) mono-static element, is the NATO research vessel Alliance, which deployed a source and a receiver buoy. The two other elements are receiver buoys forming multi-static stations. The positions of the elements is determined by differential GPS.

Each buoy contains a receiving array formed of 25 calibrated hydrophones on five bars in a star shaped form. A digital compass is used to determine the orientation allowing beamforming relative to the North. The 3-dB beamwidth of the receiver is 7° at 3500 Hz, 9° at 2700 Hz and 13° at 1900 Hz.

We analyze data at three frequencies, 1900 Hz, 2700 Hz and 3500 Hz. The data have already been analyzed for crossfixing multi-static target contacts [1].

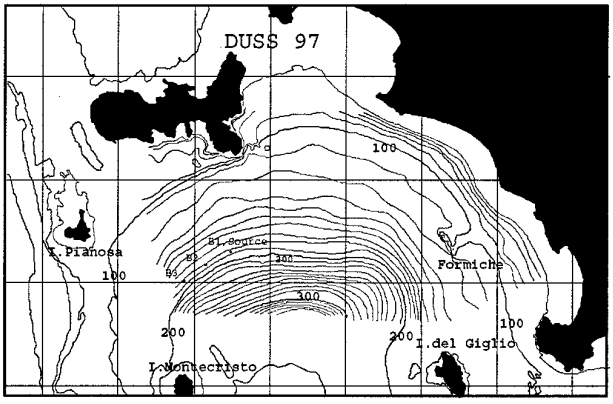

Figure 1 *Geographical map of test area, showing bottom bathymetry and deployment positions of sonar elements.*

3
Method

3.1 Signal and information processing

As mentioned above each receiving array consists of 25 calibrated hydrophones on five bars in a star shaped form. A digital compass is used to determine the orientation allowing beamforming relative to the North. The 3-dB beamwidth of the receiver is 7° at 3500 Hz, 9° at 2700 Hz and 13° at 1900 Hz. The received data were beamformed into beams spaced equally in degrees at 2° interval resulting in oversampled beams.

Compass bias due to assembly of the compass to the buoy frame may produce positioning errors [1]. These errors can be partially corrected by comparing arrival angle from a reference object with a known position. For the standalone buoys two and three we use the direct arrival of the transmitter pulse, for the mono-static buoy one the return from an Echo Repeater.

The compass readings can vary strongly even within the time of one ping, especially for buoy one which is attached to the moored ship and is thus following its movements. Therefore the compass readings are smoothed by a moving average filter and used by the beamformer. The average compass correction is about 5° with a standard deviation of 0.4°.

After the compass correction the data are mapped onto a geographic map. The average over all the pings in a run is formed to identify objects of interest, i.e. which are detected for most of the pings.

Objects to be analyzed are normalized using an analysis window around the object. Values inside this window which are below a threshold are considered background noise. The threshold is chosen to be 6 dB below the maximum value inside the object. All cells inside the analysis window are divided by the average power of the noise cells leading to normalized acoustic values in SNR.

The normalized data are smoothed by a 500 ms moving average filter. A pixel is detected if it's SNR exceeds a minimum threshold. Objects are formed of detection pixels connected over range and/or bearing[2]. For the object the following features are determined:

- position of the maximum SNR
- barycentre, in time and bearing, of the object, weighted by SNR
- total energy of the object
- size of the object, both in time and bearing

The barycentre of the object can be used as an "aiming point" [2]. It will be used to represent the object.

4

Results

In the beamformer the compass bias is corrected leading to beams pointing in absolute directions. All pings are added to form an average sonar image. An example for run 2501 is shown in Fig. 2 superimposed on a geographical bathymetry map. The average image does not show clearly visible target-like clutter. Extended reverberation features are visible for the Montecristo island in the south and an upslope bathymetry feature just south of Elba island.

4.1 Run 2501

Run 2501 used a 1 sec 200 Hz bandwidth LFM pulse at 2700 Hz centre frequency. We study two objects, returns from the Montecristo island and from an upslope bottom feature north-west of the Alliance.

The compass errors for buoy 2 and 3 were corrected against the direct arrival of the transmitted source pulse. The small distance between the source and buoy 1 did not allow the compass errors to be corrected.

The results are presented in a series of plot. For all plots the term detection is used to denote the centre of gravity of the detected object. Figure 3 shows the results for the Montecristo island. Each plot shows the average sonar output over the entire run with the barycentres of detected objects superimposed. Figures 3(a)-3(c) show the results for buoy 1 to buoy 3, Fig. 3(d) shows the detections from all buoys superimposed on the average sonar output of buoy 1. The buoy 1 detections are indicated by the brown circles, those of buoy 2 by green squares and those of buoy 3 by red triangles.

Figures 4 and 5 show the extent of the detected object in range and bearing as a function of ping number. The symbols are as in Fig. 3. Figure 6 shows the cross fixing of detections of the three buoys, for each ping the distance between the detections of the three buoys is plotted. The distance between the detections of buoy 1 and buoy 2 are plotted as brown circles, those of buoy 1 and buoy 3 as green squares and those of buoy and buoy 3 as red triangles.

The detections show, as can be expected, considerable spread in beam but less so

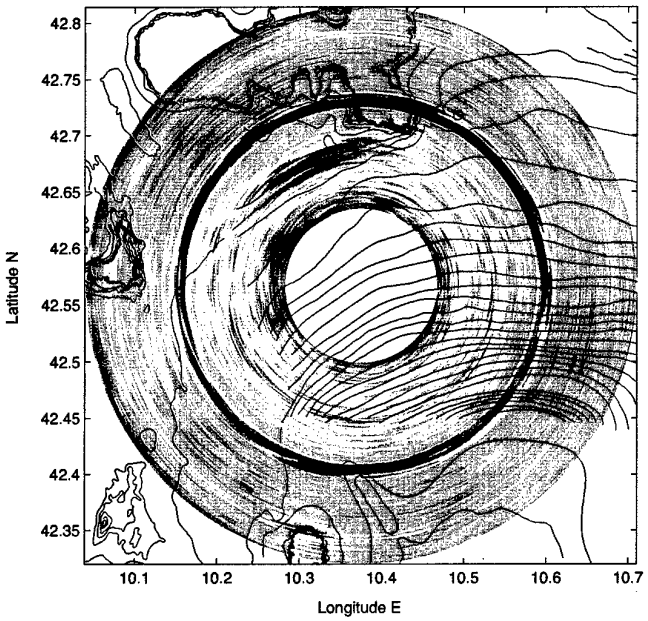

Figure 2 *Average sonar picture for run 2501.*

in range. The main source of the spread is the limited accuracy of the compass corrections. Another source is the highlight structure of the reverberation feature. Figure 7 illustrates the effect, the feature consists of two main highlights. Depending on the depth of the "valley" between the highlights and the detector's threshold the two peaks will form either one connected object or two disconnected ones. Figure 7(a) and 7(b) show examples of disconnected peaks with the upper one identified as the feature. The other possibilities are the lower peak identified as the feature (Fig. 7(c)) and the two peaks connected (Fig. 7(d)). The latter one leads to a barycentre midway between the peaks.

The separation between the two highlights is due to the large size of the reverberation feature. Smaller target-like clutter will most likely not show such a distinct highlight structure. A detector like the Page test [3] is able to join the highlights into one connected object. The Page test detector was not used in this work.

Figures 8 to 11 show the results for the upslope bathymetry feature. The symbols are as in Figs. 3 to 6. This feature is more extended in beam. Again the influence of highlight structure on detection spread is present.

4.2 Run 2506

Run 2506 used a 1 sec 200 Hz bandwidth LFM pulse at 1900 Hz centre frequency. It was executed on the same day as run 2501. For this run we only study returns from the Montecristo island.

Again the compass errors for buoy 2 and 3 were corrected against the direct arrival of the transmitted source pulse and for buoy 1 the compass errors could not be corrected.

The results are in Figs 12 to 15 .

4.3 Run 0103

Run JUL0103 used a 1 sec 200 Hz bandwidth LFM pulse at 3500 Hz centre frequency. It was executed about a week after runs 2501 and 2506. Also for this run we only study returns from the Montecristo island. During this run an Echo Repeater was active. The compass errors for all buoys were corrected against the arrival of the Echo Repeater pinger. Because buoy 1 was attached to the moored ship it is moving strongly and not all of the movements can be corrected leading to a larger spread.

The results are in Figs 16 to 19 .

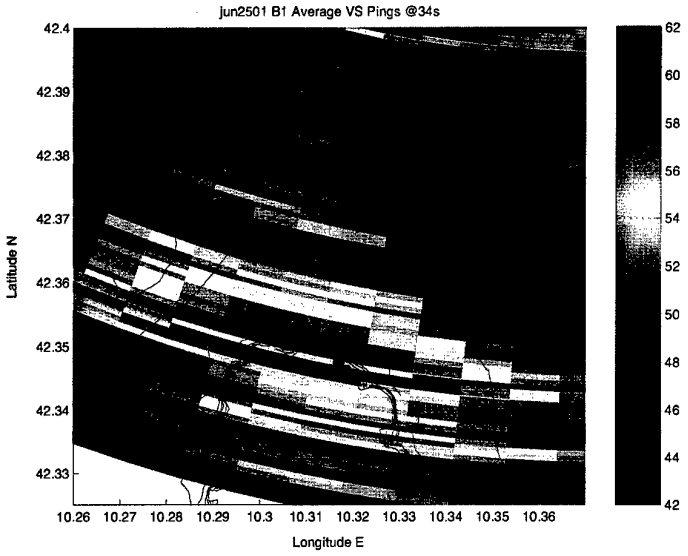

(a) buoy 1

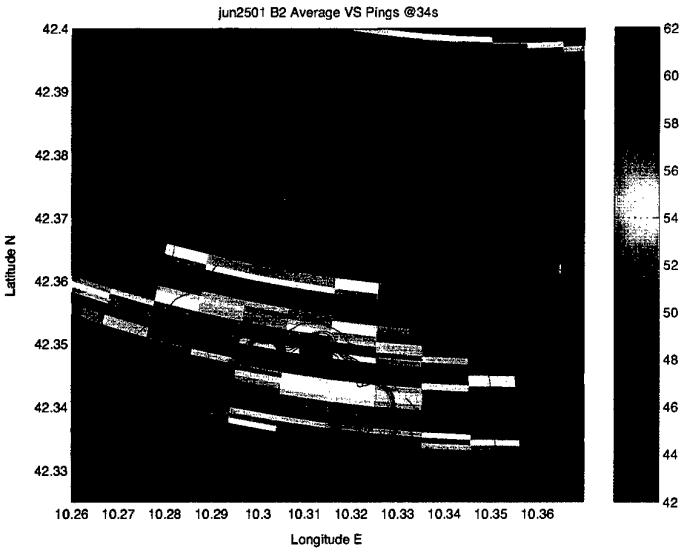

(b) buoy 2

Figure 3 *Run 2501, feature A. The centre of gravity of the detected objects is plotted over the average sonar picture for the entire run. The buoy 1 detections are indicated by the brown circles, those of buoy 2 by green squares and those of buoy 3 by red triangles.*

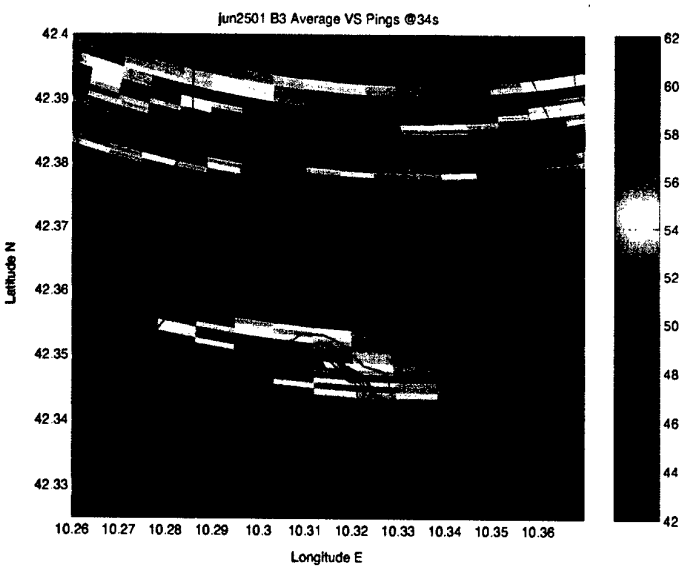

(c) buoy 3

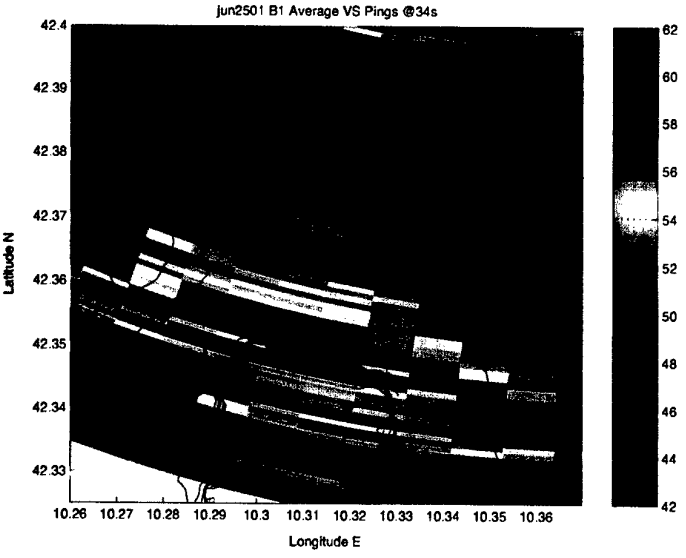

(d) all buoys

Figure 3 *Run 2501, feature A (continued).*

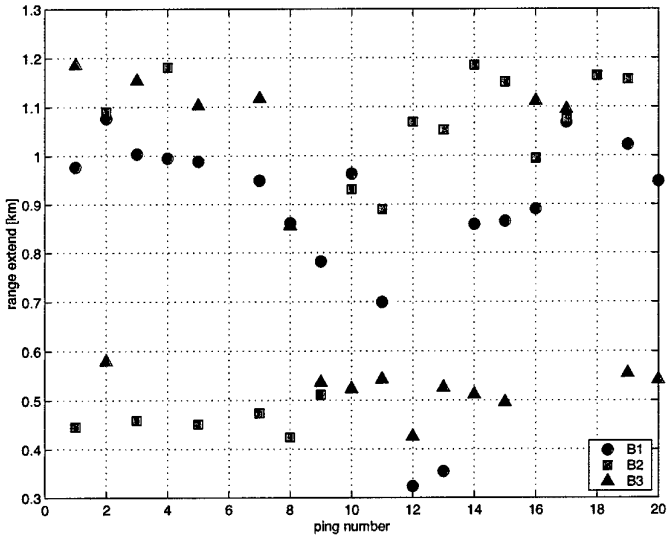

Figure 4 *Run 2501, extent in range of detected object as a function of ping number, feature A. The buoy 1 detections are indicated by the brown circles, those of buoy 2 by green squares and those of buoy 3 by red triangles.*

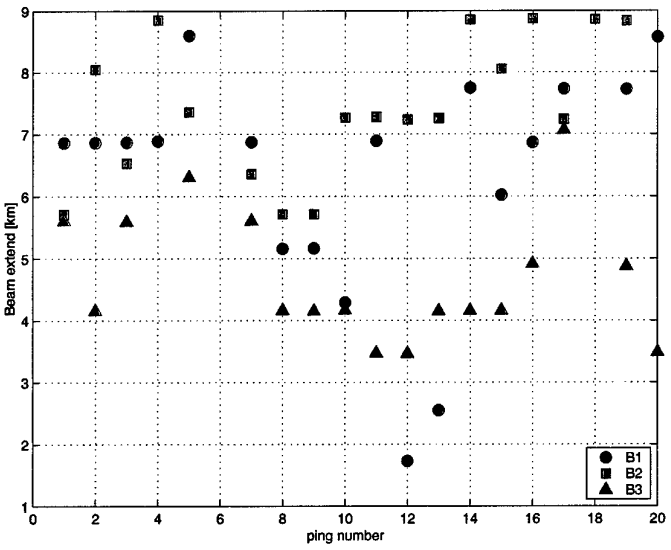

Figure 5 *Run 2501, extent in beam of detected object as a function of ping number, feature A. The buoy 1 detections are indicated by the brown circles, those of buoy 2 by green squares and those of buoy 3 by red triangles.*

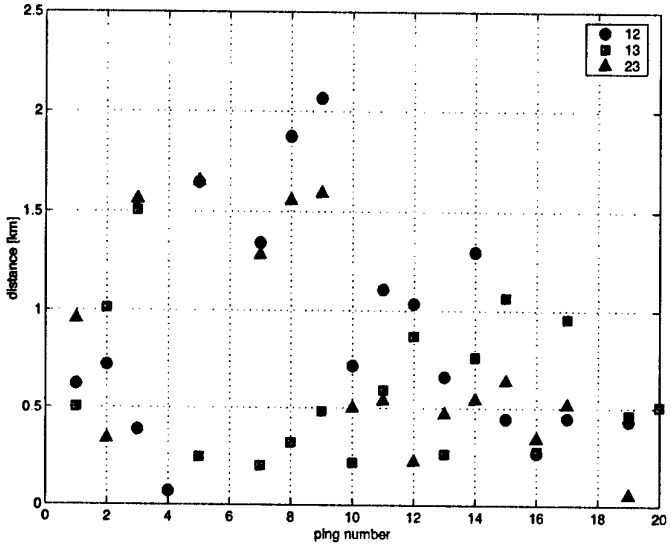

Figure 6 *Run 2501, crossfixing accuracy, feature A. For each ping the distance between the detections of the three buoys is plotted. The distance between the detections of buoy 1 and buoy 2 are plotted as brown circles, those of buoy 1 and buoy 3 as green squares and those of buoy and buoy 3 as red triangles.*

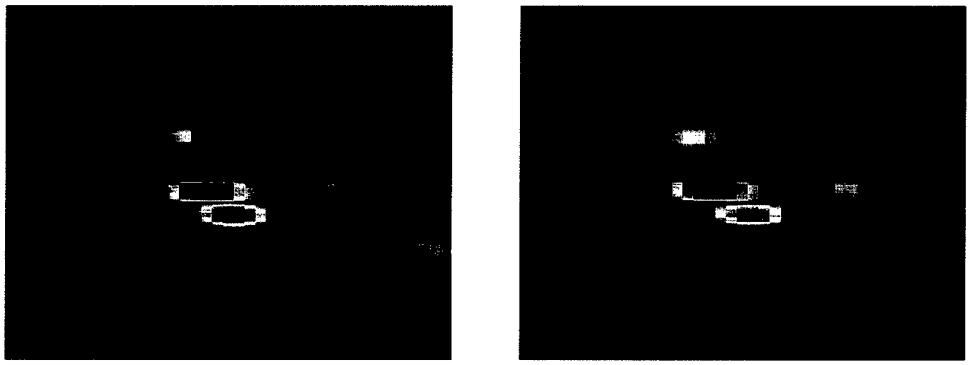

(a) ping 331

(b) ping 338

(c) ping 341

(d) ping 356

Figure 7 *Run 2501, effects of highlight structure, feature A.*

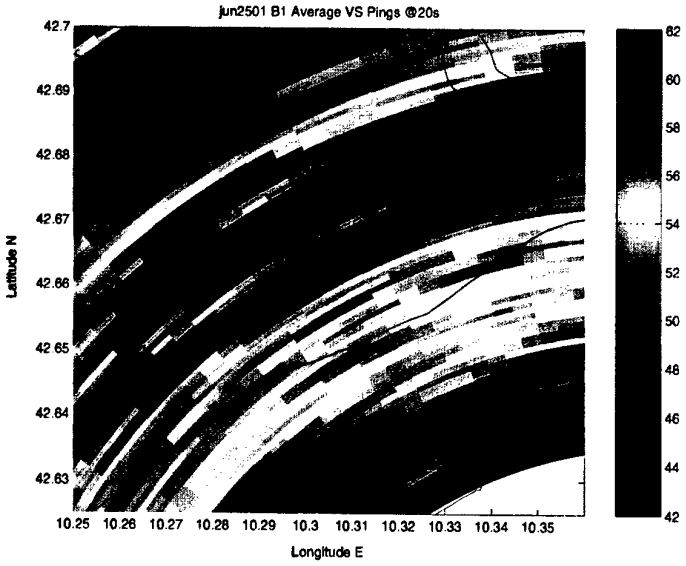

(a) buoy 1

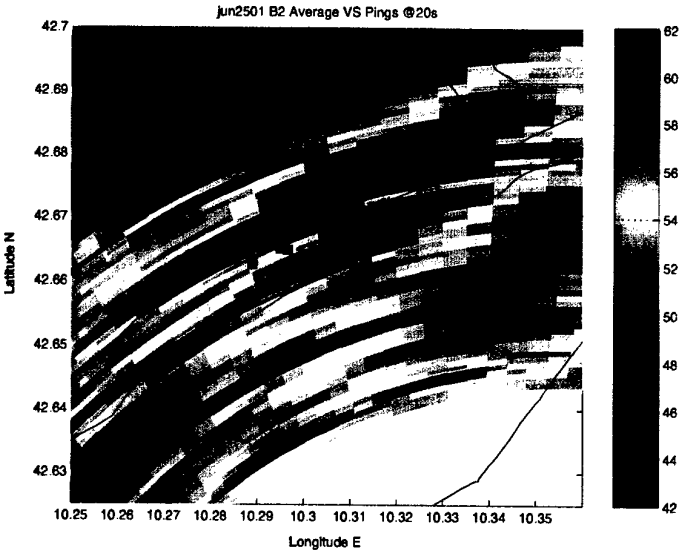

(b) buoy 2

Figure 8 *Run 2501, feature B. The centre of gravity of the detected objects is plotted over the average sonar picture for the entire run. The buoy 1 detections are indicated by the brown circles, those of buoy 2 by green squares and those of buoy 3 by red triangles.*

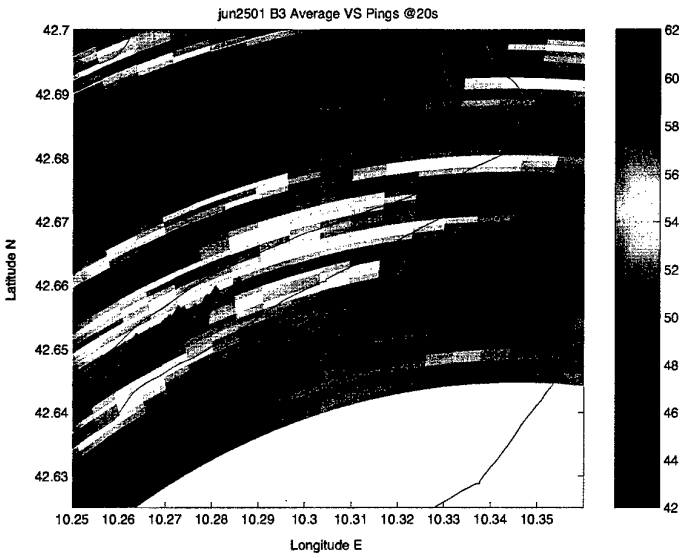

(c) buoy 3

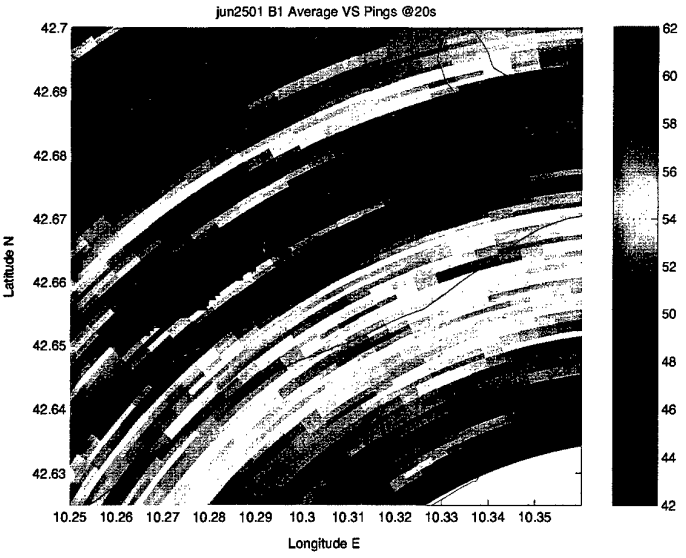

(d) all buoys

Figure 8 *Run 2501, feature B, (continued).*

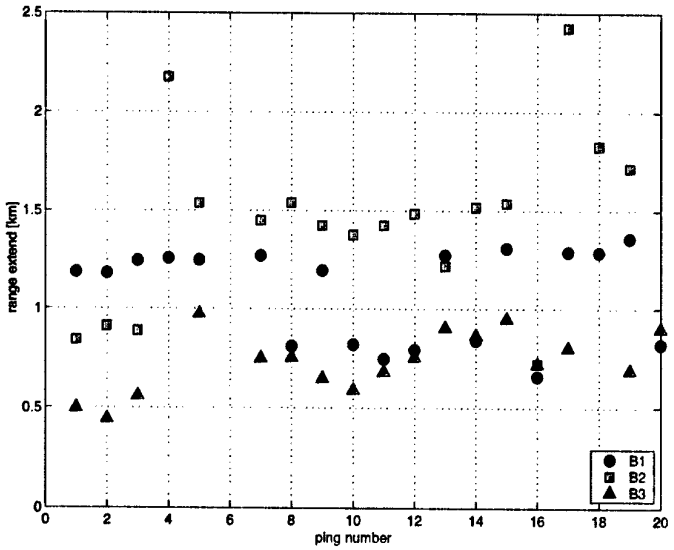

Figure 9 *Run 2501, extent in range of detected object as a function of ping number, feature B. The buoy 1 detections are indicated by the broum circles, those of buoy 2 by green squares and those of buoy 3 by red triangles.*

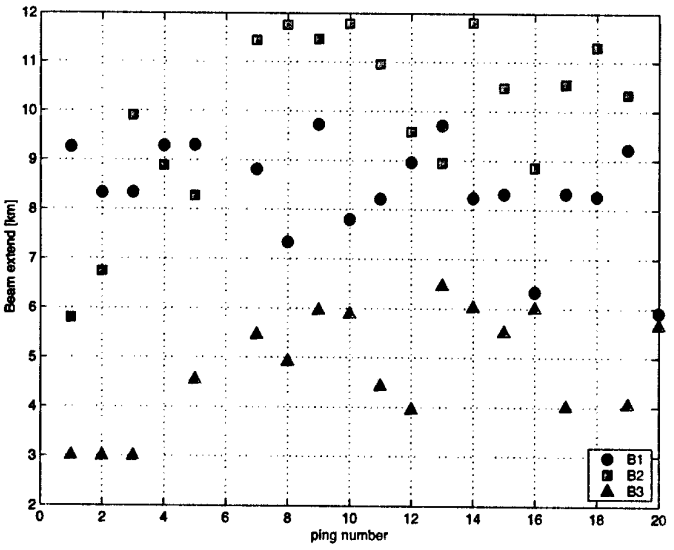

Figure 10 *Run 2501, extent in beam of detected object as a function of ping number, feature B. The buoy 1 detections are indicated by the brown circles, those of buoy 2 by green squares and those of buoy 3 by red triangles.*

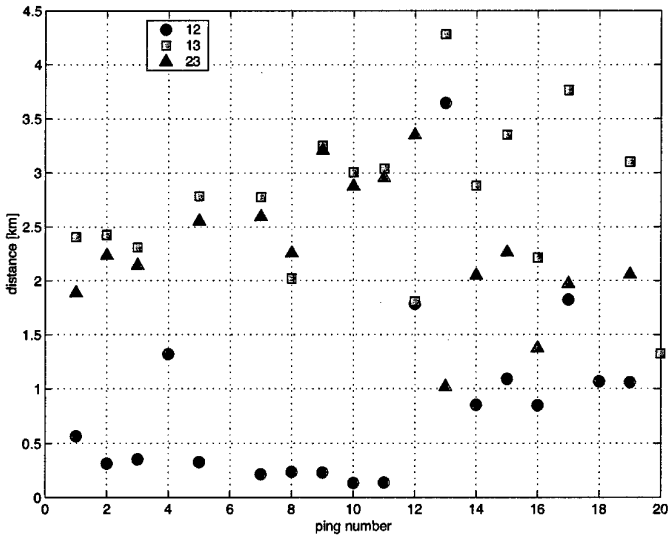

Figure 11 *Run 2501, crossfixing accuracy, feature B. For each ping the distance between the detections of the three buoys is plotted. The distance between the detections of buoy 1 and buoy 2 are plotted as brown circles, those of buoy 1 and buoy 3 as green squares and those of buoy and buoy 3 as red triangles.*

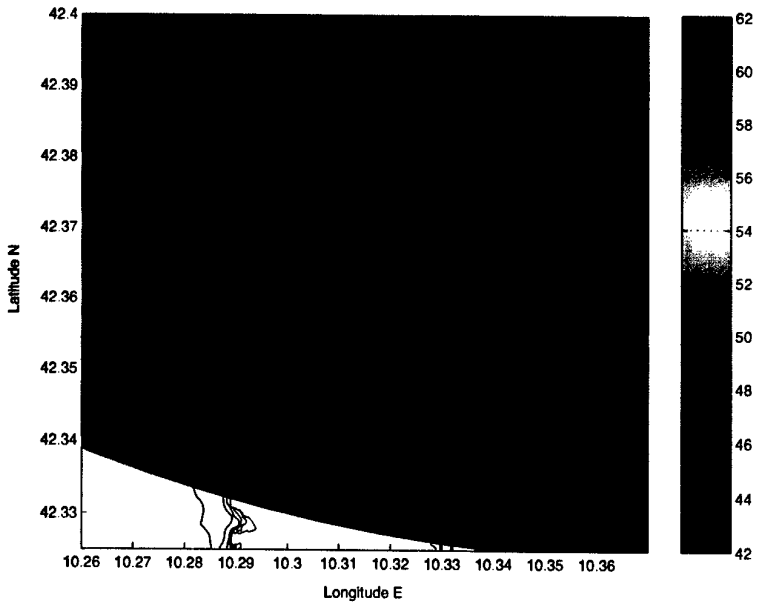

(a) buoy 1

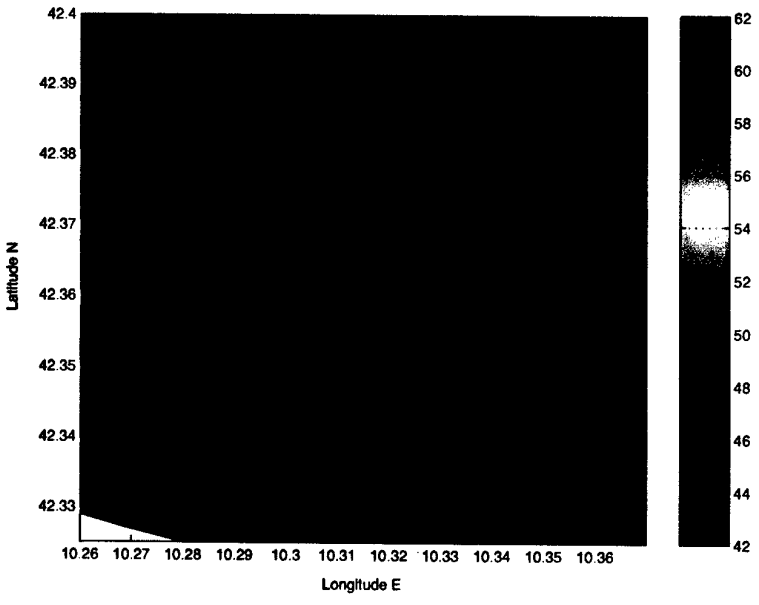

(b) buoy 2

Figure 12 *Run 2506. The centre of gravity of the detected objects is plotted over the average sonar picture for the entire run. The buoy 1 detections are indicated by the brown circles, those of buoy 2 by green squares and those of buoy 3 by red triangles.*

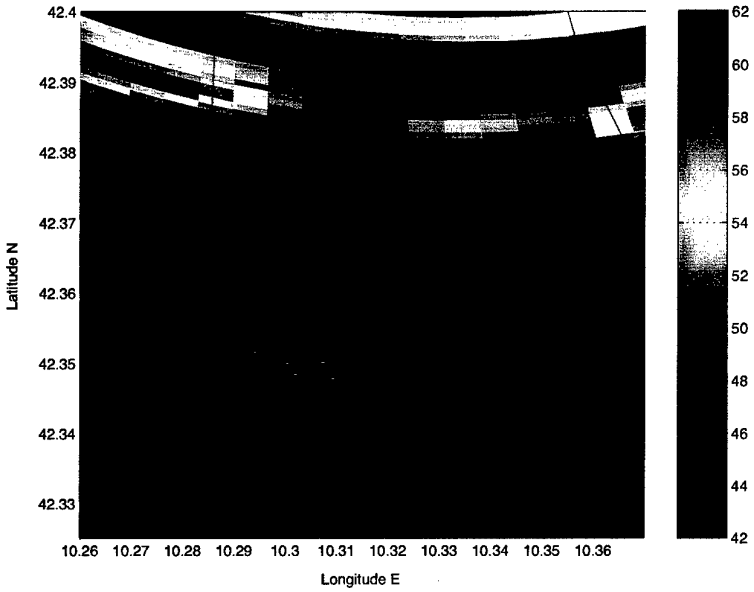

(c) buoy 3

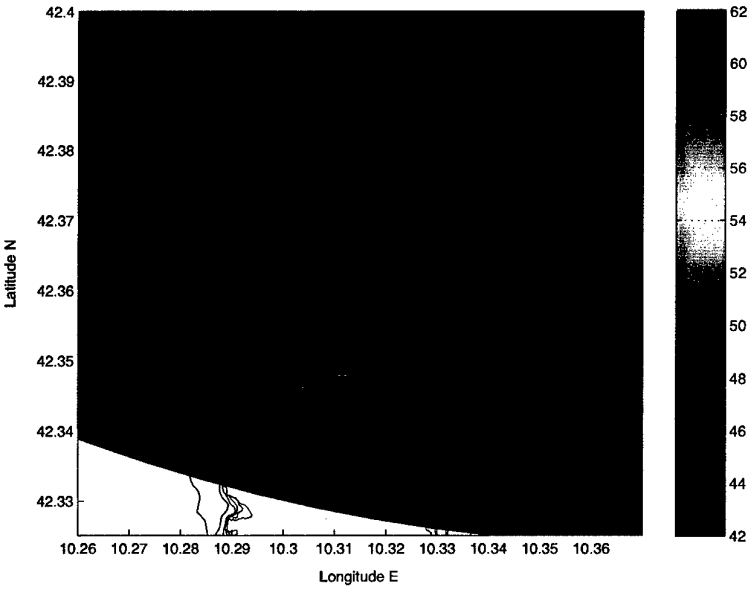

(d) all buoys

Figure 12 *Run 2506, (continued).*

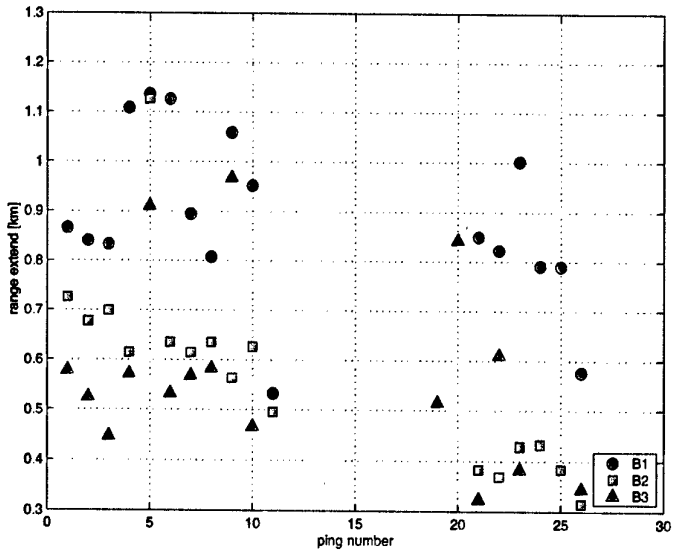

Figure 13 *Run 2506, extent in range of detected object as a function of ping number. The buoy 1 detections are indicated by the brown circles, those of buoy 2 by green squares and those of buoy 3 by red triangles.*

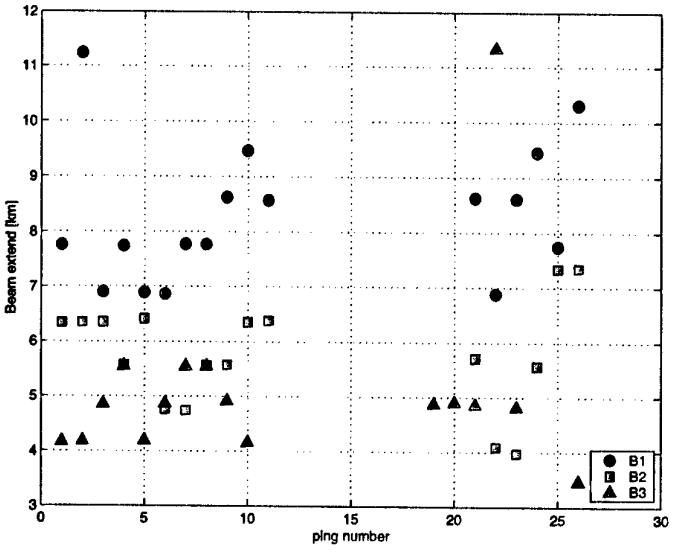

Figure 14 *Run 2506, extent in beam of detected object as a function of ping number. The buoy 1 detections are indicated by the brown circles, those of buoy 2 by green squares and those of buoy 3 by red triangles.*

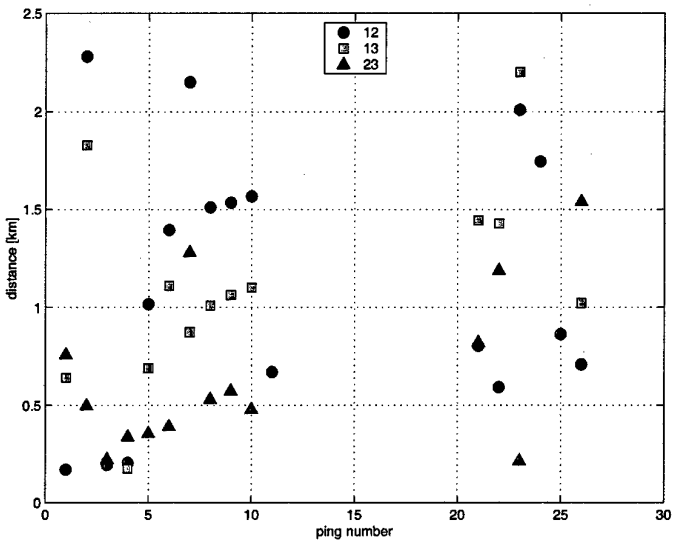

Figure 15 *Run 2506, crossfixing accuracy. For each ping the distance between the detections of the three buoys is plotted. The distance between the detections of buoy 1 and buoy 2 are plotted as brown circles, those of buoy 1 and buoy 3 as green squares and those of buoy and buoy 3 as red triangles.*

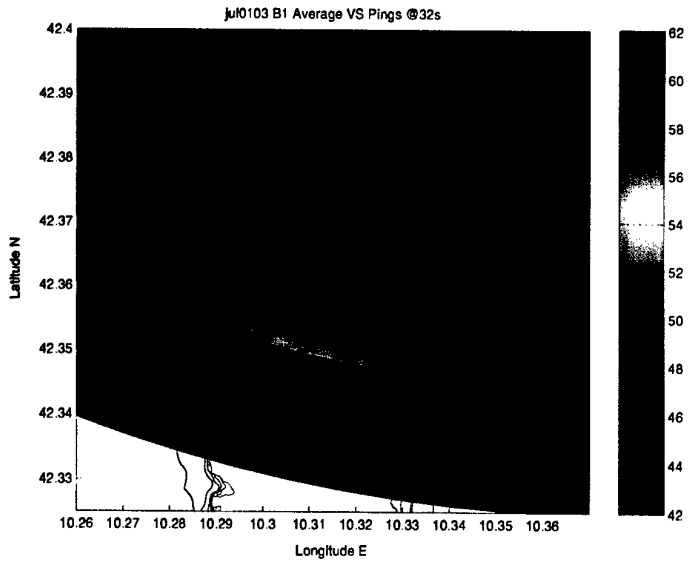

(a) buoy 1

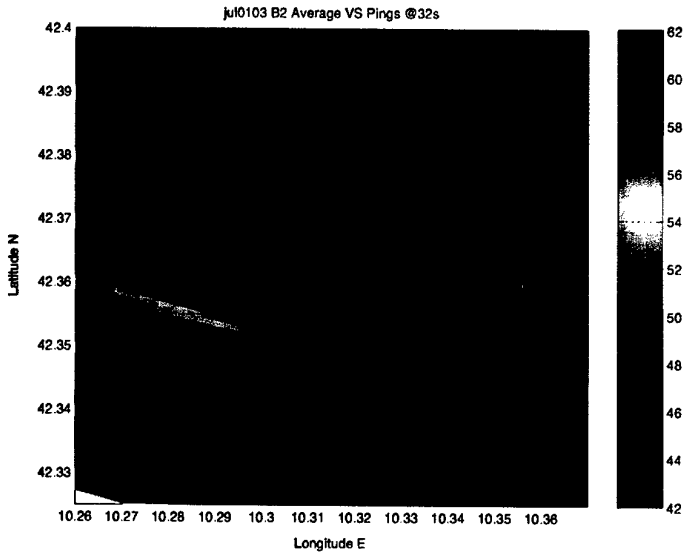

(b) buoy 2

Figure 16 *Run 0103. The centre of gravity of the detected objects is plotted over the average sonar picture for the entire run. The buoy 1 detections are indicated by the brown circles, those of buoy 2 by green squares and those of buoy 3 by red triangles.*

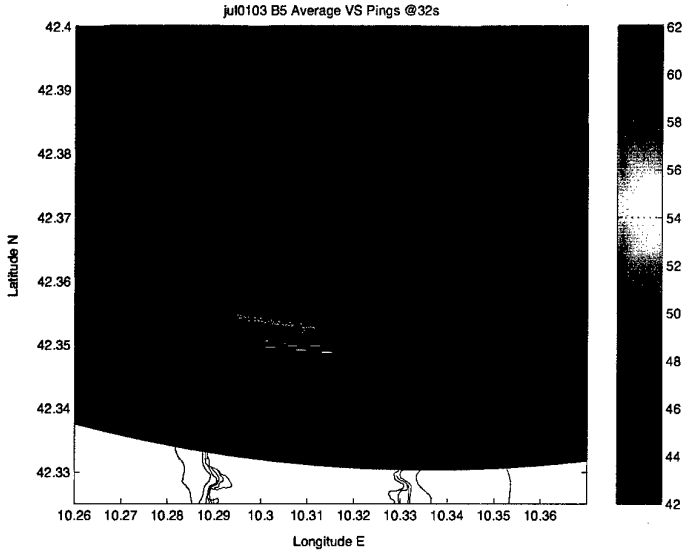

(c) buoy 3

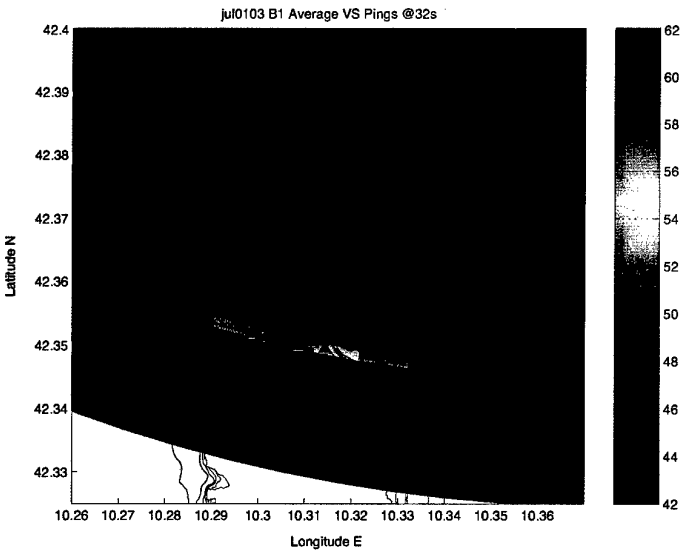

(d) all buoys

Figure 16 *Run 0103, (continued).*

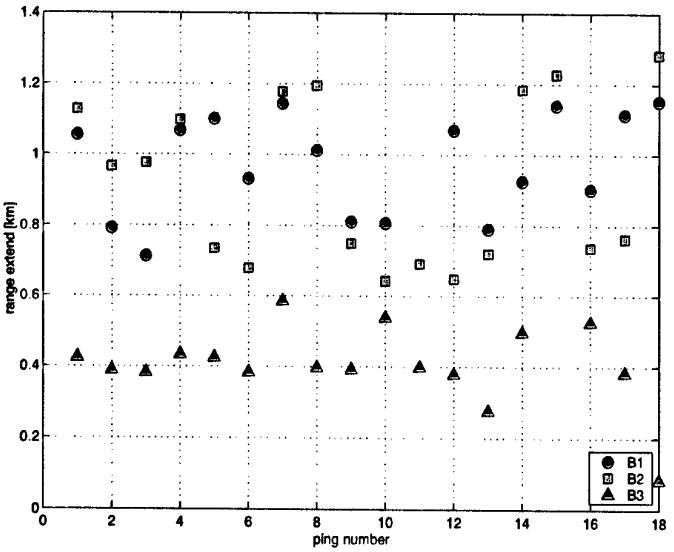

Figure 17 *Run 0103, extent in range of detected object as a function of ping number. The buoy 1 detections are indicated by the brown circles, those of buoy 2 by green squares and those of buoy 3 by red triangles.*

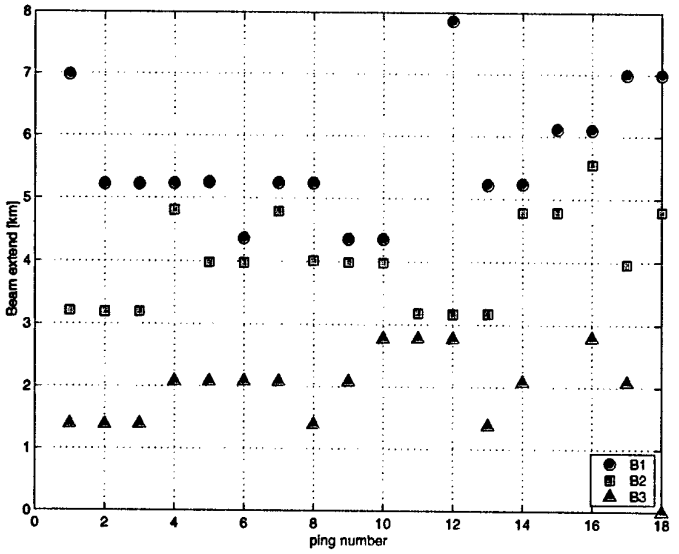

Figure 18 *Run 0103, extent in beam of detected object as a function of ping number. The buoy 1 detections are indicated by the brown circles, those of buoy 2 by green squares and those of buoy 3 by red triangles.*

4.4 Run 0307

Run 0307 used a 2 sec CW pulse with frequency 1900 Hz. This run is only included for reference as a CW pulse cannot be used to accurately localize objects. The detections are spread out in both beam and range (Fig. 20). Of course Doppler information should be used to remove fixed objects.

4.5 Crossfixing

The strength of multi-statics is that it has multiple views on objects. An object might be detected on one station when the other ones cannot see it. When an object is detected by more than one station fusion of the contacts might lead to additional information.

Figures 6, 11, 15 and 19 show the cross fixing of detections of the three buoys, for each ping the distance between the detections of the three buoys is plotted. The brown circles shows the distance between detections from buoy 1 and buoy 2, the green squares between buoy 1 and 3 and the red triangles between buoy 2 and 3.

The distance between the detections ranges from a few hundred meters to a couple of km. The larger distances are mainly due to one buoy performing worse than the other two. For example for run 0103 (Fig. 19) the distance between detections for buoy 2 and 3 are, for most pings, below 500 m. The distances to buoy 1 detections fluctuate heavily mainly because the compass corrections for this buoy are not accurate.

4.6 Frequency consistency

Table 1 summarizes the maximum distances between detections for each run and buoy. No significant difference between the runs can be noticed. Only run 0103 shows smaller spread for buoys 2 and 3. This might be due to the higher frequency, 3500 Hz *versus* 1900 Hz and 2700 Hz, but might also be a consequence of the different compass calibration. For run 0103 the compass was calibrated against arrivals of an Echo Repeater. Runs 2501 and 2506 did not use the Echo Repeater and were calibrated by the direct arrival of the transmitted signal. For these runs the compass of buoy 1 could not be corrected.

Also some buoys show a single outlier, see for example Fig. 13(c). Removing this outlier significantly reduces the spread of the detections.

To draw conclusions on frequency dependence of reverberation localization more data is needed.

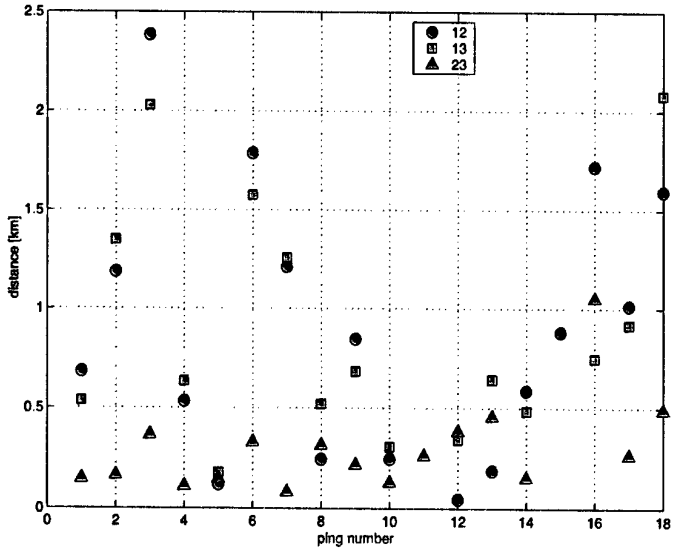

Figure 19 *Run 0103, crossfixing accuracy. For each ping the distance between the detections of the three buoys is plotted. The distance between the detections of buoy 1 and buoy 2 are plotted as brown circles, those of buoy 1 and buoy 3 as green squares and those of buoy and buoy 3 as red triangles.*

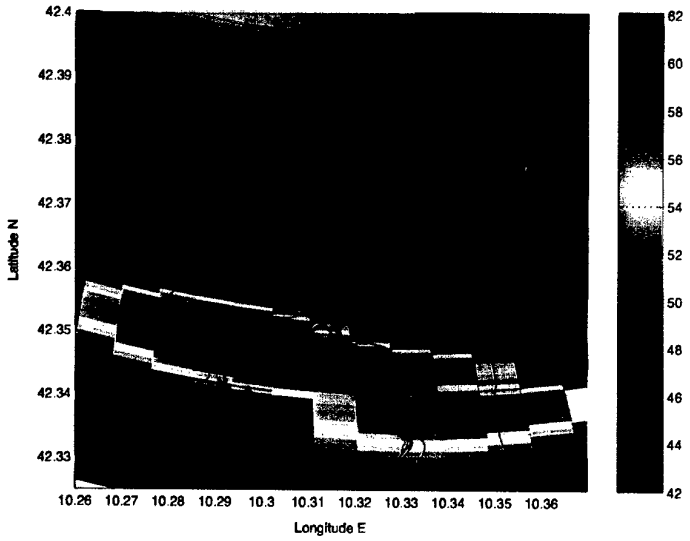

Figure 20 *Run 0307, buoy 3.*

Run	Frequency	Buoy 1	Buoy 2	Buoy 3
2501 feature A	2700 Hz	2.50 km	2.25 km	3.02 km
2501 feature B	2700 Hz	2.84 km	3.16 km	2.05 km
2506	1900 Hz	2.50 km	2.25 km	3.02 km
0103	3500 Hz	2.52 km	1.23 km	0.86 km

Table 1 *Maximum distances of detections.*

5
Conclusions

We studied the consistency of reverberation returns from the DUSS97 experiment.

The detections from reverberation features were clustered into objects and projected on a geographical map. Detected objects were represented by their centre of gravity. An attempt was made to correct the bias in the buoy's compass using known objects, the direct arrival of the source pulse and the return of an echo repeater. Even so errors in the localization remain especially for buoy 1 which was connected to the moored ship.

This localization error turns out to be the main limiting factor in the reverberation consistency. For runs where the compass errors could be accurately estimated the centres of gravity of the detected objects from different stations are a few hundred meters apart, even though the detected objects themselves are several kilometers large.

Also highlight structure influences the position of the detected objects. Clustering techniques like the Page test detector might merge the different highlights into one single object.

The present data set does not allow conclusions on the frequency dependence of the reverberation detections. Limited conclusions were made on the buoy to buoy cross fixing. More data is needed to study these effect better.

The DUSS97 experiment used three fixed receiving stations. Future work will study data acquired with a towed array. These data will show different sources of localization error. The CERBERUS01 experiment, to be held in August 2001, will acquire data from three ships with towed arrays allowing also the multi-static aspect to be studied.

References

[1] Mozzone, L., and Bongi, S. Deployable underwater surveillance systems. Localization and fusion of multistatic contacts. Evaluation of feasibility using experimental data. SR-291, SACLANTCEN, 1998.

[2] van Velzen, M., and Laterveer, R. Measuring detection performance in active sonar using object counting. SR-331, SACLANTCEN, 2001.

[3] Abraham, D., and Willett, P. Active signal detection in shallow water using the Page test. SR–252, SACLANTCEN, 1996.

Document Data Sheet

Security Classification		Project No.
UNCLASSIFIED		04-AB
Document Serial No.	**Date of Issue**	**Total Pages**
SR-348	March 2002	35 pp.

Author(s)

Laterveer, R., Bongi, S.

Title

Reverberation consistency: DUSS-97 data

Abstract

The use of low frequency active sonar in shallow water leads to large numbers of reverberation detections which can overload automatic tracking and classification algorithms.

We study the stability of reverberation returns from the DUSS97 multistatic experiment using fixed buoys.

The main conclusion is that to associate detections over station and time accurate geographical mapping of the data is essential. Therefore fixed buoys should have accurate calibrated compasses.

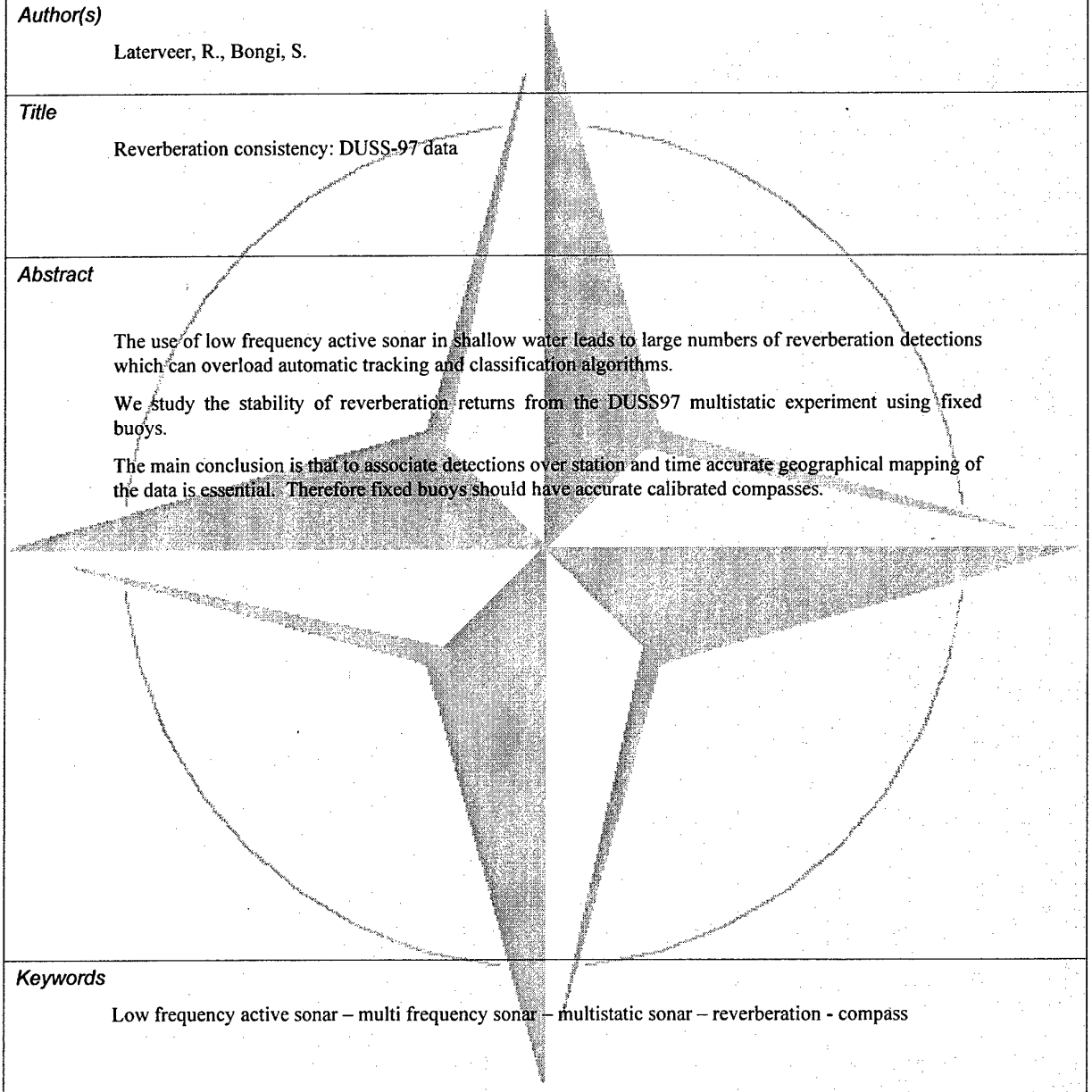

Keywords

Low frequency active sonar – multi frequency sonar – multistatic sonar – reverberation - compass

Issuing Organization

North Atlantic Treaty Organization
SACLANT Undersea Research Centre
Viale San Bartolomeo 400, 19138 La Spezia, Italy

[From N. America: SACLANTCEN (New York) APO AE 09613]

Tel: +39 0187 527 361
Fax:+39 0187 527 700

E-mail: library@saclantc.nato.int

The SACLANT Undersea Research Centre provides the Supreme Allied Commander Atlantic (SACLANT) with scientific and technical assistance under the terms of its NATO charter, which entered into force on 1 February 1963. Without prejudice to this main task - and under the policy direction of SACLANT - the Centre also renders scientific and technical assistance to the individual NATO nations.

This document is approved for public release.
Distribution is unlimited

SACLANT Undersea Research Centre
Viale San Bartolomeo 400
19138 San Bartolomeo (SP), Italy

tel: +39 0187 527 (1) or extension
fax: +39 0187 527 700

e-mail: library@saclantc.nato.int

NORTH ATLANTIC TREATY ORGANIZATION